Cerebellar white matter disruption in Alzheimer's Disease patients: a Diffusion Tensor Imaging study

Article (Unspecified)

Cerebellar white matter disruption in AD patients: a Diffusion Tensor Imaging study

Sofia Toniolo[1,2], Laura Serra[1], Giusy Olivito[1], Carlo Caltagirone[2,3], Nicola B. Mercuri[2], Camillo Marra[4], Mara Cercignani[5], Marco Bozzali[1,5]

[1]Neuroimaging Laboratory, Fondazione Santa Lucia, IRCCS, Rome, Italy.

[2]Department of Neuroscience, University of Rome 'Tor Vergata', Rome, Italy

[3]Department of Clinical and Behavioural Neurology, Fondazione Santa Lucia, IRCCS, Rome, Italy.

[4]Institute of Neurology, Catholic University, Rome, Italy.

[5]Department of Neuroscience, Brighton and Sussex Medical School, University of Sussex, Falmer, East Sussex, UK.

Running Title: Cerebellar WM damage in AD

Correspondence to: Prof. Marco Bozzali, Department of Neuroscience, Brighton and Sussex Medical School, University of Sussex, Brighton, East Sussex, BN1 9RH, UK. Telephone number: +44(0) 1273 873509; Fax number: +44 (0) 1273 876721; E mail address: m.bozzali@bsms.ac.uk

Abstract

The cognitive role of the cerebellum has recently gained much attention, and its pivotal role in Alzheimer's disease (AD) has now been widely recognized. Diffusion Tensor Imaging (DTI) has been used to evaluate the disruption of the microstructural milieu in AD, and though several white matter (WM) tracts such as corpus callosum, inferior and superior longitudinal fasciculus, cingulum, fornix and uncinate fasciculus have been evaluated in AD, data on cerebellar WM tracts are currently lacking.

We performed a tractography-based DTI reconstruction of the middle cerebellar peduncle (MCP), and the left and right superior cerebellar peduncles separately (SCPL and SCPR) and addressed the differences in fractional anisotropy (FA), axial diffusivity (Dax), radial diffusivity (RD) and mean diffusivity (MD) in the three tracts between 50 patients with AD and 25 healthy subjects (HS).

We found that AD patients showed a lower FA and a higher RD compared to HS in MCP, SCPL and SCPR. Moreover, a higher MD was found in SCPR and SCPL and a higher Dax in SCPL. This result is important as it challenges the traditional view that WM bundles in the cerebellum are unaffected in AD and might identify new targets for therapeutic interventions.

Keywords: AD, diffusion tensor imaging, white matter, probabilistic tractography, cerebellum.

Introduction

Alzheimer's Disease (AD) has been classically regarded as a neurodegenerative disorder primarily affecting the grey matter (GM) [1]. Nevertheless, white matter (WM) alterations in AD have gained increasing attention in recent years, and Diffusion Tensor Imaging (DTI) has been widely used in clinical research settings for its ability to detect microstructural damage even at its earliest stages, when atrophy is still undetectable [1-5]. Tightly packed axons and myelin sheaths in the brain restrict the free motion of water molecules, leading to anisotropic diffusion according to the orientation of axonal bundles. In AD this neat microstructural milieu is disrupted, leading to a loss of anisotropic diffusion due to small vessel alterations, demyelination of axonal structures, degradation of microtubules, loss of axonal structure and gliosis [6]. DTI is used to examine these microscopic alterations to quantify the breakdown of tissue's fine-grain architecture. This implies the fitting of the diffusion-weighted signal to a simple tensor model, mathematically represented as an ellipsoid at the voxel level [7]. Diffusion along the major axis of the ellipsoid is termed axial diffusivity (Dax), whereas the average of the second and third minor axes is called radial diffusivity (RD) and reflects diffusivity perpendicular to the major axis of the tensor [8]. Moreover, mean diffusivity (MD) is calculated from the average of the three values, indicating the magnitude of overall water diffusion in each voxel, independently of the directionality [8]. In AD an increase in Dax, MD and RD have been widely reported [9,10], and each metric provides us with unique information as they might change in different directions along disease progression [11]. Increased Dax and MD are considered to be the first abnormalities to occur but they remain relatively static throughout the time course of the disease, and therefore could be used as 'state-specific' markers [11,12]. In contrast, RD becomes increasingly abnormal with disease progression, and has been regarded as 'stage-

specific' marker [11]. Another important 'stage-specific marker' is fractional anisotropy (FA), which represents the fraction of the tensor that can be assigned to anisotropic diffusion, with values closer to zero reflecting more isotropic diffusion, and therefore typically higher microstructural damage [13]. Indeed, DTI is especially valuable to tackle AD in its earliest phase, and this technique has proven to be sensitive even in mild cognitive impairment (MCI) patients [6,14,15], and moreover, a valuable tool in predicting conversion from MCI to AD [6,16,17]. A lower FA has been previously reported in several WM bundles in the AD population [9,17-19], and correlates clinically with disease severity and neuropathologically with the presence of higher Braak neurofibrillary tangle (NFT) stage (Braak stages V-VI) in the ventral cingulum tract, entorhinal cortex, and white matter adjacent to the precuneus [19]. A reduction in FA and an increase of Dax, MD and RD in AD patients have been described in the corpus callosum, inferior and superior longitudinal fasciculus, cingulum, fornix and uncinate fasciculus [3, 8, 9, 11], but at the present time no studies specifically focused on cerebellar WM tracts are available.

The cerebellum was regarded for decades as being purely involved in motor tasks control. Nevertheless, thanks to the ground-breaking work by Schmahmann and Sherman in 1998 [20] nowadays its role in cognitive and affective disorders is well established. The selective damage of the vermis and posterior lobe of the cerebellum has been related to the so called "cerebellar cognitive affective syndrome" (CCAS), namely a subset of symptoms including impairment of executive functions such as planning and set-shifting, verbal fluency, abstract reasoning, working memory, visual-spatial organization and even personality change [20]. Moreover, deficits in executive function, attentional processes, working memory and divided attention have been described after microsurgical treatment of tumours or hematomas in the cerebellum

[21]. The posterior lobules of the cerebellum have been related to cognitive tasks such as verb generation, mental rotation, and working memory [22,23] through several fMRI studies and show highly specific functional connections to areas of the default mode network (DMN) such as posterior cingulate, the lateral temporal cortex, the inferior parietal lobule, and an extended region along medial prefrontal cortex [24], which are key regions for AD connectivity and structural changes [25,26]. Within the posterior lobes, Crus I has shown to be functionally correlated to the DMN [27], and show the highest degree of atrophy among cerebellar regions [27,28]. Nevertheless, data on cerebellar WM tract involvement in AD is currently unavailable. Given these recent findings related to the involvement of the cerebellum in AD, the aim of our work was to investigate the DTI microstructural fibre integrity of the cerebellar WM tracts in AD patients compared to healthy subjects (HS), and to establish the relationship between WM and GM damage. The middle (MCP) and superior cerebellar peduncles (SCP) are the main WM bundles connecting the cerebellum with the cerebrum, being respectively the main input and output connections to/from the cerebellum [29]. Here, we reconstructed the middle cerebellar peduncle (MCP), and the left and right superior cerebellar peduncles separately (SCPL and SCPR) [30] and addressed the differences in FA, Dax, RD and MD in the three tracts between AD patients and HS.

Materials and methods

Participants

Seventy-five subjects were recruited from the Dementia unit of the Catholic University, Rome, Italy. Among the participants, 50 subjects had a diagnosis of AD according to the IWG-2 Criteria of 2014 [31], while 25 were age-matched healthy subjects who

served as controls. All patients had typical AD with an amnestic profile. None of the HS showed evidence of cognitive deficits on neuropsychological testing. All subjects underwent a complete clinical investigation, including medical history, neurological examination, a complete blood test screening (including routine exams, thyroid function tests, and levels of B_{12} and folate). Exclusion criteria for all subjects included contra-indication for magnetic resonance imaging (MRI), previous history of alcohol or substance abuse, focal brain lesions on brain imaging, significant neurological or psychiatric history and the presence of major systemic illness.

Subjects were excluded if they had two or more hyperintense lesions > 10 mm, or more than eight hyperintense lesions between 5 and 9 mm to exclude prominent vascular damage.

The study was approved by the Ethical Committee of Santa Lucia Foundation and written informed consent was obtained from all participants before study initiation. All procedures performed in this study were in accordance with the 1964 Helsinki declaration and its later amendments or comparable ethical standards.

Neuropsychological assessment

All patients underwent a complete Neuropsychological battery before MRI scanning. MMSE was performed for assessing general cognitive status [32], Rey 15-Words List Immediate recall (cut-off ≥ 28.5) and Delayed recall (cut-off ≥ 4.6) [33] for verbal episodic long-term memory, Copy of drawings (cut-off ≥ 7.1) [33] and Copy of drawings with landmarks (cut-off ≥ 61.8) [33] for praxis, Digit span forward (cut-off ≥ 3.7) and backward [34] for verbal short term memory and Corsi blocking task forward (cut-off ≥ 3.5) and backward [34] for visuo-spatial short term memory, Phonological Word Fluency (cut-off ≥17.3) [33] for executive functions, Naming of

objects (cut-off ≥ 22) [35] for language skills. Each test was adjusted for gender, age and education for the neuropsychological statistical analyses.

MRI data acquisition

All imaging was obtained using a 3.0 T MR scanner (Siemens Allegra, Erlangen, Germany), equipped with a circularly polarized transmit-receive coil. The maximum gradient strength is 40 mT^{-1}, with a maximum slew rate of 400 $mT\ m^{-1}$, ms^{-1}. The following scans were collected from each studied subject: dual echo turbo spin echo (TSE) (TR = 6190 ms, TE = 12/109 ms), fast fluid attenuated inversion recovery (FLAIR) (TR = 8170 ms, TE = 96 ms), 3D modified driven equilibrium Fourier transform (MDEFT) scan (TR = 1338 ms, TE = 2,4 ms, Matrix = 256 x 224 x 176, in-plane FOV = 250 x 250 mm^2, slice thickness 1 mm), diffusion weighted Spin-Echo Echo Planar Imaging (SE EPI) (TR = 7 s, TE = 85 ms, maximum b factor = 1000 s mm^2, isotropic resolution = 2.3 mm^3). This sequence collects seven images with no diffusion weighting (b0) and 61 images with diffusion gradients applied in 61 noncollinear directions. According to the inclusion criteria, TSE and FLAIR scans were reviewed to assess the presence of remarkable macroscopic brain abnormalities. Images were processed to obtain measures of atrophy (GM and WM volumes) and microstructural damage (FA, MD, Dax, RD).

White matter analysis

The cerebellum was pre-processed individually in SPM-8 (http://www.fil.ion.ucl.ac.uk/spm/), using "SUIT", a dedicated toolbox that allows to extract and normalize the GM and WM from the cerebellum. SUIT is a toolbox designed to align the infratentorial anatomy of the brain to a dedicated spatially

unbiased template of the human cerebellum and brainstem. , Through automated nonlinear normalization methods, provides a more accurate intersubject-alignment than current whole-brain methods [36].

T1 weighted volumes were segmented fully into GM and WM, prior to normalisation to a cerebellar focused SUIT template. This procedure allows more accurate co-registration, and hence may allow a better WM specific analysis of volume loss. Images were smoothed using a 8-mm FWHM Gaussian kernel according to Dayan et al [30].

Tractography

The MCP and SCP were reconstructed following the methods described by Dayan et al [30]. The main orientation in every voxel was determined according to the multi-fiber directions estimated in each voxel from the fiber orientation distribution functions (fODFs) calculated with either Q-ball imaging [37] or persistent angular structure (PAS) MRI [30,38]. The fODF calculation method chosen depended on the curvature and amount of crossing of each WM tract. Since Q-ball, compared with PAS, tends to provide fewer false-positive fiber components while dealing less effectively with fiber crossing, it was used for the MCP reconstruction. Conversely, since the SCP is particularly difficult to reconstruct in the brain stem where it decussates, the PAS method was chosen for this tract. Once the multi-fiber directions had been estimated, probabilistic tractography was carried out based on these data using the probabilistic index of connectivity (PICo) algorithm. The PICo algorithm [39], implemented in CAMINO (www.camino.org.uk), assigns to every voxel in the brain a probability of being connected to the seed point by considering multiple pathways emanating from the seed-point region and from each point along the reconstructed pathways. The probability is estimated by streamline-based tracking

iterations repeated in a Monte Carlo fashion, and the effect of noise is estimated through a calibration step. Streamlines that do not reach the way-point regions are discarded. N = 10000 tracking iterations were performed from each voxel of the seed region of interest (ROI) applying a stopping threshold of FA ≤ 0.1 and an angle threshold of 80°. The fiber directions in every voxel were changed for each iteration according to the uncertainty associated with their estimation. Among these iterations, only tracts going through "waypoint" ROIs were selected. An "end-point" ROI pair was used, so as to retain only tracts where each extremity reached one of the two different end-point ROIs. Finally, tracts intersecting "exclusion" ROIs were removed and a probability map was calculated so that the PICo value of each voxel was equal to the number of remaining tracts intersecting that voxel, divided by the total number of iterations.

Middle cerebellar peduncle analysis

For the MCP, the seed was placed bilaterally in a single coronal plane, just anterior to the dentate nucleus of each cerebellar hemisphere, in regions with fibers with anterior-posterior orientation (green in color-coded FA maps). Generated tracts were made to pass through two coronal waypoint ROIs placed bilaterally, and anteriorly, to each seed ROI. Finally, an exclusion ROI was placed in an axial plane above the pons to prevent the tracts from ascending superiorly to that level.

Superior cerebellar peduncle analysis

The SCP was segmented separately for each cerebellar hemisphere. For the left SCP (L-SCP), defined as originating from the left cerebellar hemisphere, the seed was placed on a single coronal slice in the dentate nucleus. We chose seed voxels whose principal direction of diffusion was not towards neighboring voxels belonging to the

MCP. A pair of endpoint ROIs was drawn so that the first ROI was just posterior to the seed ROI (so as to select all the fibers that continue posteriorly), and the second ROI was placed contralaterally to include both the red nucleus and its medial area, which the SCP is known to pass through.

Two exclusion ROIs were further delineated: one in the whole coronal slice immediately superior to the second end-point ROI and another in a sagittal plane so as to extend superiorly up to a few voxels below the known SCP decussation. ROIs sagittally symmetrical to the ones just described were used for the right SCP (R-SCP).

The group-average MCP, L-SCP and R-SCP maps were calculated independently using the following procedure: first, the individual tract PICo maps were thresholded at a value chosen to minimize the amount of volume variation depending on the PICo threshold. The curve representing the volume as a function of the PICo threshold varied; the curve vertex was estimated for each subject by estimating the smallest radius of curvature, after which the median among all subjects was selected as the common threshold to be applied to all PICo maps. Second, once the binarized individual maps had been obtained, the FA to MNI transformation was applied to these maps to provide a group-average map in MNI space. Finally, the subject-count threshold chosen to obtain a binary map of the "average tract" was set visually as the maximum, which provided a reconstruction matching known neuroanatomy. This threshold was set to 50% for the MCP, L-SCP and R-SCP tracts.

Statistical analysis

VBM and DTI analysis

A between-group voxel-wise comparison of the WM volume was performed within the framework of Voxel-Based-Morphometry (VBM). A mask of every tract of interest was created from the results of tractography averaged across the whole population. The VBM analysis was then restricted to this region of interests using SPM and a one way ANOVA model. Regional differences and correlations were considered significant only if they survived after correction for multiple comparisons (Family wise error, FWE correction at cluster-level, $p < 0.05$). Age, gender and education were included as covariates of no interest in the analysis. The same statistical analysis was performed on DTI metrics, with the exception of additionally adding also tract volumes as covariates of no interest. This allows an unbiased assessment of measures of microscopic tissue integrity.

We performed a partial correlation statistical analysis between neuropsychological parameters and DTI metrics using raw scores and DTI values as variables, and age, gender, education, and tract volumes as covariates.

Results

AD patients and HS were not statistically different in terms of age but different in terms of education ($p = 0.0005$) and gender distribution ($p = 0.02$), so we included the latter variables as covariates of no interest in the voxel-wise analysis.

Neuropsychological testing

As expected, AD patients showed a statistically lower MMSE score compared to HS, as well as lower scores in all other neuropsychological tests (Table 1), placing them as a group at a moderate stage of severity. As shown by the results of neuropsychological testing (Table 1), they had significant memory impairment (e.g.

very low delayed recall at Rey 15 words), with a relative relative sparing of verbal fluency.

White matter VBM analysis and DTI-based Tractography

We found no significant differences between AD and HS in terms of WM volumes in the cerebellar VBM analysis. MCP and SCPL were successfully reconstructed in 75 participants, while SCPR were artifact-free only for 72 participants. Overview of the three reconstructed tracts is shown in Figure 1A. The MCP included the transverse pontine fibers posterior and anterior to the corticospinal tracts (Figure 1B, red overlay), while the SCP featured a visible decussation at the level of the midbrain: SCPL (Figure 1B, yellow overlay), SCPR (Figure 1B, light blue overlay).

Voxel-wise analysis of cerebellar WM microstructural parameters

AD patients showed lower FA and higher RD values compared to HS in MCP, SCPL and SCPR. Moreover, a higher MD was found in SCPR and SCPL and a higher Dax in SCPL (Table 2). We found no correlation between Neuropsychological tests and FA, MD, Dax or RD values.

Post-hoc correlations between DTI values and GM atrophy

In order to establish any association between GM and WM degeneration in the cerebellum of people with AD, we performed a voxel-based analysis on the correlation between the DTI indices found to be abnormal in the main analysis, and and grey matter volumes of the cerebellum. This analysis was performed in Alzheimer's disease patients only. We found that the reduction in FA of the MCP seen in AD is correlated to GM atrophy in Lobule IX ($p = 0.023$) (Figure 2). No other

significant associations where found in the other diffusivity metrics in MCP and in SCPR and SCPL.

Discussion

An emerging body of literature targeting specifically the cerebellum with the newly developed SUIT atlas [36] has shown how GM loss involving predominantly Crus I is a rather specific finding in AD [27, 40], but data on selective WM loss are currently lacking. Using SUIT-VBM, sensitive to macroscopic tissue loss, we found no evidence of WM loss in MCP, SCPL and SCPR in AD patients compared to HS. By contrast, we found widespread microstructural changes, as measured by diffusion MRI indices. As often demonstrated, this result confirms that changes in microstructural diffusion metrics are independent from WM atrophy in AD brains [41]. Moreover, it supports the concept that microstructural alterations may be detected earlier than macroscopic WM volume loss in AD, and may be predictive of accumulation of atrophy along the disease progression [41-43].

Admittedly, a previous study [44] has reported areas of WM loss in AD patients compared to HS. However, there are some methodological differences with our current study, including the absence of DTI tract reconstruction and cerebellar VBM parcellation (using the SUIT), and recruitment of patients at a more advanced disease stage. This might account for the detection of atrophy that we did not find in our current study.

However,The meaning of changes in FA, MD, Dax and RD must be interpreted cautiously because diffusivity changes may be influenced by GM and WM atrophy [49]. For minimizing the effects of this potential bias we used tract volumes as a covariate in our analysis. In our study, FA and RD represent the more reliable metric

to assess WM cerebellar damage, which showed a significant alteration in all the three tracts examined. Lower FA in middle cerebellar peduncle in AD is in line with previous findings [43], though an increased RD (typically associated with demyelination) has not been yet specifically reported.

A higher MD was found in SCPR and SCPL, although in our sample we were not able to detect it in MCP, and this might require further investigations.

Dax was found significantly higher in SCPL but not in SCPR, where it showed a p-value just above the significance threshold ($p = 0.07$). This might be partially due to a less efficient reconstruction of SCPR (accounting for 72 over 75 patients).

The relative poorer performance of Dax compared to FA could be explained by the fact that cerebellar WM bundles are characterized by a higher proportion of crossing fibers with respect to the cerebrum, and DTI metrics are highly affected by vectors modifications in areas of kissing, fanning and crossing fibers [50] such as SCPL and SCPR decussations or MCP median crossing bundles. Dax is especially unreliable because the single cylindrical model of white matter fibers is violated [50-51]. We tried to compensate this methodological constraint by using two different estimation procedures for MCP and SCP, using PAS in the SCP because it allows a better reconstruction in areas of fiber crossing such as the brainstem where SCPL and SCPR decussate. A clearer interpretation of our findings in terms of AD pathology could be given by comparing the changes in DTI indices with markers of amyloid deposition, as suggested by previous literature [52]. Unfortunately, this was not possible in the present study, since CSF analysis or Amyloid PET was not performed, thus preventing a more in-depth understanding of the relationship between the progression of WM cerebellar change and the underlying amyloid pathology. This is especially important with respect to aging population. In healthy aging, regions which show a

reduction in FA in middle age largely overlap with regions that exhibit volume loss in older age suggesting that microstructural FA changes may precede and predict volume loss [42]. We did, however, examine the relationship between WM microstructural damage and cerebellar GM atrophy. In our study, the reduction in FA of the MCP seen in AD correlated with GM atrophy in Lobule IX, which is a cerebellar region associated within the Default Mode Network according to Buckner et al [24]. This network is selectively impaired in AD patients [24]. The presence of a significant correlation does not inform us about the causality of these processes, but indicates that damage in the 2 tissues might accumulate at a similar pace. The lack of significant results with SCPL and SCPR should be interpreted with caution, due to the small size of these tracts.

We failed to identify any association between standard neuropsychological tests and DTI metrics. One possible explanation relies on the specificity of the neuropsychological evaluations used in this study. Distinct WM bundles of the brain are related to different cognitive functions. Damage of fornix, cingulum, genu and splenium of the corpus callosum have been related to global cognitive decline [53]. Temporal lobe and posterior cingulate WM damage have been linked to poor delayed recall performance [54], and similar correlations were found between the frontal WM and executive function [55] and the posterior part of the corpus callosum and verbal fluency [56]. None of the neuropsychological tests in our studies are specifically targeted to cerebellar cognitive functions, so further assessments will be required to draw a linear correlation between DTI metrics in the cerebellum and cognitive performances on neuropsychological testing.

Moreover, the majority of GM studies involving the cerebellum failed in identifying associations between areas of GM loss and scores at neuropsychological standard tests [40]. A newly developed scale for cerebellar cognitive functions has been recently introduced [57], though it has no Italian validation yet, and future study will determine its usefulness in clinical and research practice.

A secondary aim of our study was to see whether the cerebellar WM would be selectively affected in AD. MCP and SCP diameters have recently been included in the EFNS/MDS-ES guidelines in the differential diagnosis among different movement disorders' syndromes such as Progressive Supranuclear Palsy (PSP), Multiple system atrophy (MSA), Parkinson's Diseade (PD) and Cortico Basal Degeneration (CBD) [58], with a reduced MCP diameter <8.0 mm being rather specific for MSA [59]. Stating that AD patients do not show WM atrophy compared to healthy controls might be of relevance in this context, though a direct comparison between MSA and AD patients would be advisable. A reduced FA in MCP is another common finding in MSA. This has been previously observed not only in MSA-C but also in MSA-P [60], and has also been used to differentiate between MSA-C and cerebellar degenerative ataxias [47].

Moreover, diffusivity changes in SCP have been regarded as a marker that can point the diagnosis towards PSP instead of PD (Level B recommendation of the EFNS/MDS-ES guidelines) [58].

We therefore proved that even in AD, DTI metrics in the cerebellum are altered, challenging the traditional assumptions that these tracts are preserved in AD. Interestingly, these results could offer new potential therapeutic strategies, since the cerebellum is a brain structure easily reachable with non-invasive brain stimulation tools, which have already proven to have clinical efficacy in other neurodegenerative

disorders [61-62]. Moreover, another study showed that stimulation of the cerebellum can have beneficial effects in restoring altered intracortical circuitry in AD patients [63].

In conclusion, this study confirms the importance of DTI in assessing AD patients because even when macrostructural alterations such as VBM-detectable atrophy cannot not be traced, diffusion based alterations are already present. Stating the breakdown of both input and output connections between the cerebellum and the cerebrum is important in the view of the role of the cerebellum in both feedback and feedforward cognitive processing [64].

Moreover, our results highlight the involvement of WM tracts in AD patients, which could be traced not only in brain regions that are traditionally regarded as highly affected in AD patients, but also in the cerebellum, a yet underestimated cognitively relevant brain region. The importance of the cerebellar involvement in AD patients is in line with a large body of literature [65] and should be taken into account when relating to AD pathological macro and microstructural changes.

References

1. Bozzali M, Serra L, Cercignani M. Quantitative (2016) MRI to understand Alzheimer's disease pathophysiology. *Curr Opin Neurol* **29**, 437-444.
2. Scola E, Bozzali M, Agosta F, Magnani G, Franceschi M, Sormani MP, Cercignani M, Pagani E, Falautano M, Filippi M, Falini A (2010) A diffusion tensor MRI study of patients with MCI and AD with a 2-year clinical follow-up. *J. Neurol Neurosurg Psychiatry* **81**, 798–805.
3. Bozzali M, Giulietti G, Basile B, Serra L, Spanò B, Perri R, Giubilei F, Marra C, Caltagirone C, Cercignani M (2012) Damage to the cingulum contributes to alzheimer's disease pathophysiology by deafferentation mechanism *Hum Brain Mapp* **33**, 1295-1308.
4. Gold BT, Johnson NF, Powell DK, Smith CD. (2012) White matter integrity and vulnerability to Alzheimer's disease: preliminary findings and future directions. *Biochim Biophys Acta* **1822**, 416–422.
5. Giulietti G, Torso M, Serra L, Spanò B, Marra C, Caltagirone C, Cercignani M, Bozzali M, Alzheimer's Disease Neuroimaging Initiative (ADNI). (2018) Whole brain white matter histogram analysis of diffusion tensor imaging data detects microstructural damage in mild cognitive impairment and Alzheimer's disease patients *J Magn Reson Imaging* **21**, 1-13.
6. Bronge L, N. Bogdanovic N, and L. O. Wahlund LO (2002) Postmortem MRI and histopathology of white matter changes in Alzheimer brains: A quantitative, comparative study. *Dement Geriatr Cogn Disord* **13**, 205–212.
7. Oishi K, Mielke MM, Albert M, Lyketsos CG, Mori S (2011) DTI analyses and clinical applications in Alzheimer's disease. *Adv. Alzheimer's Dis* **2**, 525–534.
8. Madden DJ, Bennett IJ, Burzynska A, Potter GG, Chen NK, Song AW (2012) Diffusion tensor imaging of cerebral white matter integrity in cognitive aging. *Biochim Biophys Acta* **1822**, 386–400
9. Bozzali M, Falini A, Franceschi M, Cercignani M, Zuffi M, Scotti G, Comi G, Filippi M (2002) White matter damage in Alzheimer's disease assessed in vivo using diffusion tensor magnetic resonance imaging. *J Neurol Neurosurg Psychiatry* **72**, 742-746.
10. Henf J, Grothe MJ, Brueggen K, Teipel S, Dyrba M1 (2017) Mean diffusivity in cortical gray matter in Alzheimer's disease: The importance of partial volume correction *NeuroImage Clin* **17**, 579-586.
11. Acosta-Cabronero J, Alley S, Williams GB, Pengas G, Nestor PJ. (2012) Diffusion Tensor Metrics as Biomarkers in Alzheimer's Disease. *PLoS One* **7**, e49072.
12. O'Dwyer L, Lamberton F, Bokde AL, Ewers M, Faluyi YO, Tanner C, Mazoyer B, O'Neill D, Bartley M, Collins DR, Coughlan T, Prvulovic D, Hampel H. Multiple Indices of Diffusion Identifies (2011) White Matter Damage in Mild Cognitive Impairment and Alzheimer's Disease. *PLoS One*, **6**, e21745
13. Alba-Ferrara LM, de Erausquin GA (2013) What does anisotropy measure? Insights from increased and decreased anisotropy in selective fiber tracts in schizophrenia. *Front Integr Neurosci*, **7**, 9.
14. Lee P, Ryoo H, Park J, Jeong Y, Alzheimer's Disease Neuroimaging Initiative (2017) Morphological and microstructural changes of the hippocampus in early MCI: A study utilizing the alzheimer's disease neuroimaging initiative database. *J Clin Neurol* **13**, 144-154.
15. Nir TM, Jahanshad N, Villalon-Reina JE, Toga AW, Jack CR, Weiner MW, Thompson PM; Alzheimer's Disease Neuroimaging Initiative (ADNI) (2013)

Effectiveness of regional DTI measures in distinguishing Alzheimer's disease, MCI, and normal aging. *NeuroImage Clin* **3**, 180-195
16. Solodkin A1, Chen EE, Van Hoesen GW, Heimer L, Shereen A, Kruggel F, Mastrianni J (2013) In vivo parahippocampal white matter pathology as a biomarker of disease progression to Alzheimer's disease. *J Comp Neurol* **521**, 4300–4317.
17. Nir TM, Jahanshad N, Villalon-Reina JE, Isaev D, Zavaliangos-Petropulu A, Zhan L, Leow AD, Jack CR Jr, Weiner MW, Thompson PM; Alzheimer's Diseaase Neuroimaginng Initiative (ADNI) (2017) Fractional anisotropy derived from the diffusion tensor distribution function boosts power to detect Alzheimer's disease deficits. *Magn Reson Med* **78**, 2322–2333.
18. Mayo CD, Mazerolle EL, Ritchie L, Fisk JD, Gawryluk JR; Alzheimer's Disease Neuroimaging Initiative. (2017) Longitudinal changes in microstructural white matter metrics in Alzheimer's disease, *NeuroImage Clin,* **13**, 330–338.
19. Kantarci K, Murray ME, Schwarz CG, Reid RI, Przybelski SA, Lesnick T, Zuk SM, Raman MR, Senjem ML, Gunter JL, Boeve BF, Knopman DS, Parisi JE, Petersen RC, Jack CR Jr, Dickson DW (2017) White-matter integrity on DTI and the pathologic staging of Alzheimer's disease *Neurobiol. Aging*, **56**, 172–179.
20. Schmahmann JD and Sherman JC (1998) The cerebellar cognitive affective syndrome. Brain **121**, 561–579.
21. Gottwald B, Wilde B, Mihajlovic Z, Mehdorn HM (2004) Evidence for distinct cognitive deficits after focal cerebellar lesions. *J Neurol Neurosurg Psychiatry* **75**, 1524–1531.
22. Stoodley CJ, Valera EM, Schmahmann JD (2012) Functional topography of the cerebellum for motor and cognitive tasks: An fMRI study, *Neuroimage* **59**, 1560-1570.
23. Stoodley CJ, Valera EM, Schmahmann JD (2010) "An fMRI study of intra-individual functional topography in the human cerebellum. *Behav Neurol* **23**, 65-79.
24. Buckner RL, Krienen FM, Castellanos A, Diaz JC, Yeo BT (2011) The organization of the human cerebellum estimated by intrinsic functional connectivity. *J Neurophysiol* **106**, 2322–45.
25. Greicius MD, Srivastava G, Reiss AL, Menon V (2004) Default-mode network activity distinguishes Alzheimer's disease from healthy aging: evidence from functional MRI. *Proc Natl Acad Sci U.S.A.***101**, 4637-4642.
26. Gili T, Cercignani M, Serra L, Perri R, Giove F, Maraviglia B, Caltagirone C, Bozzali M (2011) Regional brain atrophy and functional disconnection across Alzheimer's disease evolution. *J Neurol Neurosurg Psychiatry* **82**:58-66.
27. Guo CC, Tan R, Hodges JR, Hu X, Sami S, Hornberger M (2016) "Network-selective vulnerability of the human cerebellum to Alzheimer's disease and frontotemporal dementia. *Brain* **139**, 1527-1538.
28. Toniolo S, Serra L, Olivito G, Marra C, Bozzali M, Cercignani M (2018) Patterns of Cerebellar Gray Matter Atrophy Across Alzheimer's Disease Progression. *Front Cell Neurosci* **20**;12:430.
29. Keser Z, Hasan KM, Mwangi BI, Kamali A, Ucisik-Keser FE, Riascos RF, Yozbatiran N, Francisco GE, Narayana PA (2015) Diffusion tensor imaging of the human cerebellar pathways and their interplay with cerebral macrostructure. *Front Neuroanat* **9**,41.
30. Dayan M, Olivito G, Molinari M, Cercignani M, Bozzali M, Leggio M (2016) Impact of cerebellar atrophy on cortical gray matter and cerebellar peduncles as assessed by voxel-based morphometry and high angular resolution diffusion imaging. *Funct Neurol* **31**, 239–248.

31. Dubois B, Feldman HH, Jacova C, Hampel H, Molinuevo JL, Blennow K, DeKosky ST, Gauthier S, Selkoe D, Bateman R, Cappa S, Crutch S, Engelborghs S, Frisoni GB, Fox NC, Galasko D, Habert MO, Jicha GA, Nordberg A, Pasquier F, Rabinovici G, Robert P, Rowe C, Salloway S, Sarazin M, Epelbaum S, de Souza LC, Vellas B, Visser PJ, Schneider L, Stern Y, Scheltens P, Cummings JL. (2014) Advancing research diagnostic criteria for Alzheimer's disease: The IWG-2 criteria. *The Lancet Neurology* **13**, 614–629.
32. Folstein MF, Folstein SE, McHugh PR (1975) "Mini-mental state". A practical method for grading the cognitive state of patients for the clinician. *J Psychiatr Res* **12**, 189–98.
33. Carlesimo GA, Caltagirone C, Gainotti G (1996) The mental deterioration battery: Normative data, diagnostic reliability and qualitative analyses of cognitive impairment. *Eur Neurol* **36**, 378–384.
34. Orsini A, Grossi D, Capitani E, Laiacona M, Papagno C, Vallar G (1987) Verbal and spatial immediate memory span: Normative data from 1355 adults and 1112 children. *Ital . Neurol Sci* **8**, 537–548.
35. Miceli G, Laudanna A, Burani C (1991) Batteria per l'analisi dei deficit afasici, in *Berdata*, Ass.ne per lo sviluppo delle ricerche neuropsicologiche. Berdata, Ed Milano, 1991.
36. Diedrichsen J, Balsters JH, Flavell J, Cussans E, Ramnani N (2009) A probabilistic MR atlas of the human cerebellum *Neuroimage* **46**, 39–46.
37. Hess CP1, Mukherjee P, Han ET, Xu D, Vigneron DB (2006) Q-ball reconstruction of multimodal fiber orientations using the spherical harmonic basis. *Magn Reson Med* **56**, 104–117.
38. Jansons KM1, Alexander DC (2003) Persistent angular structure: New insights from diffusion magnetic resonance imaging data. *Inverse Probl* **19**, 1031–1046.
39. Parker GJ1, Haroon HA, Wheeler-Kingshott CA (2003) A framework for a streamline-based probabilistic index of connectivity (PICo) using a structural interpretation of MRI diffusion measurements. *J Magn Reson Imaging* **18,** 242–254.
40. Gellersen HM, Guo CC, O'Callaghan C, Tan RH, Sami S, Hornberger M (2017) Cerebellar atrophy in neurodegeneration—a meta-analysis. *J Neurol Neurosurg Psychiatry* **88**, 780-788.
41. Serra L, Cercignani M, Mastropasqua C, Torso M, Spanò B, Makovac E, Viola V, Giulietti G, Marra C, Caltagirone C, Bozzali M (2016) Longitudinal Changes in Functional Brain Connectivity Predicts Conversionto Alzheimer's Disease. *J Alzheimers Dis* **51**, 377–389.
42. Hugenschmidt CE, Peiffer AM, Kraft RA, Casanova R, Deibler AR, Burdette JH, Maldjian JA, Laurienti PJ (2008) Relating imaging indices of white matter integrity and volume in healthy older adults. *Cereb Cortex* **18**, 433–442.
43. Shim G, Choi KY, Kim D, Suh SI, Lee S, Jeong HG, Jeong B1 (2017) Predicting neurocognitive function with hippocampal volumes and DTI metrics in patients with Alzheimer's dementia and mild cognitive impairment. *Brain Behav* **7**, e00766.
44. Canu E, McLaren DG, Fitzgerald ME, Bendlin BB, Zoccatelli G, Alessandrini F, Pizzini FB, Ricciardi GK, Beltramello A, Johnson SC, Frisoni GB (2010) Microstructural diffusion changes are independent of macrostructural volume loss in moderate to severe Alzheimer's disease. *J Alzheimer's Dis* **19**, 963–976.
45. Bennett IJ, Madden DJ, Vaidya CJ, Howard DV, Howard JH Jr (2010) Age-related differences in multiple measures of white matter integrity: A diffusion tensor imaging study of healthy aging *Hum Brain Mapp* **31**, 378–390.
46. Allen JS, Damasio H, Grabowski TJ, Bruss J, Zhang W (2003) Sexual dimorphism

and asymmetries in the gray-white composition of the human cerebrum. *Neuroimage* **18**, 880–894.
47. Prakash N, Hageman N, Hua X, Toga AW, Perlman SL, Salamon N (2009) Patterns of fractional anisotropy changes in white matter of cerebellar peduncles distinguish spinocerebellar ataxia-1 from multiple system atrophy and other ataxia syndromes. *Neuroimage* **47** (Suppl 2), T72-81.
48. Shin YW, Kim DJ, Ha TH, Park HJ, Moon WJ, Chung EC, Lee JM, Kim IY, Kim SI, Kwon JS (2005) Sex differences in the human corpus callosum: diffusion tensor imaging study. *Neuroreport* **16**, 795–798.
49. Salat DH, Tuch DS, Greve DN, van der Kouwe AJ, Hevelone ND, Zaleta AK, Rosen BR, Fischl B, Corkin S, Rosas HD, Dale AM (2005) Age-related changes in prefrontal white matter measured by diffusion tensor imaging. *Neurobiol Aging* **26**, 1215-1227.
50. Alexander AL, Hasan KM, Lazar M, Tsuruda JS, Parker DL (2001) Analysis of partial volume effects in diffusion-tensor MRI. *Magn Reson Med* **45**, 770–780.
51. Wheeler-Kingshott CA, Cercignani M (2009) About 'axial' and 'radial' diffusivities. *Magn Reson Med* **61**, 1255–1260.
52. Pietroboni AM, Scarioni M, Carandini T, Basilico P, Cadioli M, Giulietti G, Arighi A, Caprioli M, Serra L, Sina C, Fenoglio C, Ghezzi L, Fumagalli GG, De Riz MA, Calvi A, Triulzi F, Bozzali M, Scarpini E, Galimberti D (2018) CSF β-amyloid and white matter damage: a new perspective on Alzheimer's disease. *J Neurol Neurosurg Psychiatry* **89**, 352-357.
53. Sexton C E, Kalu UG, Filippini N, Mackay CE, Ebmeier KP (2011) A meta-analysis of diffusion tensor imaging in mild cognitive impairment and Alzheimer's disease. *Neurobiology of Aging* **32**, 2322.e5-18.
54. Goldstein FC, Mao H, Wang L, Ni C, Lah JJ, Levey AI (2009) White matter integrity and episodic memory performance in mild cognitive impairment: A diffusion tensor imaging study. *Brain Imaging Behav* **3**, 132–141.
55. Huang J, Auchus AP (2007) Diffusion tensor imaging of normal appearing white matter and its correlation with cognitive functioning in mild cognitive impairment and Alzheimer's disease. *Ann N Y Acad Sci* **1097**, 259-264.
56. Kavcic V, Ni H, Zhu T, Zhong J, Duffy CJ (2008) White matter integrity linked to functional impairments in aging and early Alzheimer's disease. *Alzheimers Dement* **4**, 381–389.
57. Hoche F, Guell X, Vangel MG, Sherman JC, Schmahmann JD (2018) The cerebellar cognitive affective/Schmahmann syndrome scale *Brain* **141**, 248–270.
58. Berardelli A, Wenning GK, Antonini A, Berg D, Bloem BR, Bonifati V, Brooks D, Burn DJ, Colosimo C, Fanciulli A, Ferreira J, Gasser T, Grandas F, Kanovsky P, Kostic V, Kulisevsky J, Oertel W, Poewe W, Reese JP, Relja M, Ruzicka E, Schrag A, Seppi K, Taba P, Vidailhet M (2013) EFNS/MDS-ES recommendations for the diagnosis of Parkinson's disease. *Eur J Neurol* **20**, 16-34.
59. Nicoletti G, Fera F, Condino F, Auteri W, Gallo O, Pugliese P, Arabia G, Morgante L, Barone P, Zappia M, Quattrone A (2006) MR imaging of middle cerebellar peduncle width: differentiation of multiple system atrophy from Parkinson disease.," *Radiology* **239**, 825-830.
60. Fanciulli A, Wenning GK (2015) Multiple-System Atrophy. *N Engl J Med* **372,** 249-263.
61. Brusa L, Ponzo V, Mastropasqua C, Picazio S, Bonnì S, Di Lorenzo F, Iani C, Stefani A, Stanzione P, Caltagirone C, Bozzali M, Koch G (2014) Theta burst stimulation modulates cerebellar-cortical connectivity in patients with

progressive supranuclear palsy. *Brain Stimul* **7**, 29-35.
62. Koch G, Porcacchia P, Ponzo V, Carrillo F, Cáceres-Redondo MT, Brusa L, Desiato MT, Arciprete F, Di Lorenzo F, Pisani A, Caltagirone C, Palomar FJ, Mir P (2014) Effects of two weeks of cerebellar theta burst stimulation in cervical dystonia patients. *Brain Stimul*. **7**, 564-72.
63. Di Lorenzo F, Martorana A, Ponzo V, Bonnì S, D'Angelo E, Caltagirone C, Koch G (2013) Cerebellar theta burst stimulation modulates short latency afferent inhibition in Alzheimer's disease patients. *Front Aging Neurosci* **5**,2.
64. Ramnani N (2006) The primate cortico-cerebellar system: Anatomy and function. *Nat Rev Neurosci* **7**, 511-522.
65. Jacobs HIL, Hopkins DA, Mayrhofer HC, Bruner E, van Leeuwen FW, Raaijmakers W, Schmahmann JD (2017) The cerebellum in Alzheimer's disease: evaluating its role in cognitive decline. *Brain* **141**, 37-47.

Table 1. Principal demographic and neuropsychological features of participants.

Demographics		**AD patients (N=50)**	**HS (N=25)**
Age		70.5 (4.5)	67.2 (6.7)
Gender distribution (M/F)		16/34 *	15/10
Years of Education		7.9 (1.6) *	12.2 (3.4)
Cognitive domain	**Neuropsychological test**		
Global cognition	MMSE	19.4 (4.2) *	28.7 (4.5)
Verbal episodic memory	Rey's 15 words list (immediate recall)	21.0 (9.6) *	43.7 (13.5)
	Rey's 15 words list (delayed recall)	1.3 (1.9) *	9.2 (3.5)
Executive functions	Phonological verbal fluency	18.4 (11.1) *	36.8 (11.7)
Short term memory	Digit span forward	4.7 (1.20) *	5.8 (1.2)
	Digit span backward	2.7 (2.0) *	4.3 (1.8)
	Corsi's blocking task forward	3.4 (1.4) *	5.0 (1.4)
	Corsi's blocking task backward	2.0 (1.7) *	4.4 (1.7)
Praxis	Drawing copy test	4.7 (3.8) *	10.7(4.1)
	Landmark drawing copy test	54.5 (16.5) *	69.4 (17.4)
Language	Naming test	19.2 (11.8) *	29.1 (12.2)

*AD versus HS, p-value<0.01.

Abbreviations: AD = Alzheimer's disease; HS = healthy subjects; MMSE = Mini-Mental State Examination. All the values are presented as follows: Mean values (SD). SD = Standard Deviation.

Table 2. Areas of microscopic white matter abnormality in AD patients compared to controls.

Structure	DTI metrix	Cluster size	Coordinates (x,y,z)			Z-score	p-value
MCP	**FA (AD<HS)**	15	16	-46	-36	5.48	0.003
		30	-18	-36	-40	4.55	0.000
		29	28	-54	-36	4.43	0.000
		29	28	-42	-42	4.41	0.000
		37	20	-44	-34	4.27	0.000
		24	22	-46	-32	4.06	0.000
		17	-30	-42	-40	3.99	0.000
SCPL	**RD (AD>HS)**	11	18	-32	-38	3.65	0.031
	Dax (AD>HS)	34	-4	-40	-26	5.20	0.000
	FA (AD<HS)	13	-8	-50	-32	4.55	0.001
		12	-14	-48	-32	4.48	0.002
		6	-4	-40	-28	4.00	0.013
SCPR	**MD (AD>HS)**	29	-4	-40	-26	5.50	0.000
		8	8	-34	-16	3.80	0.014

RD (AD>HS)	31	-4	-40	-26	5.53	0.000
	4	8	-34	-16	3.41	0.036
FA (AD<HS)	4	10	-54	-32	4.11	0.025

Abbreviations: AD = Alzheimer's disease; HS = healthy subjects; MCP= Medial Cerebellar Peduncle; SCP= Superior Cerebellar Peduncle; R=Right; L=Left.

Cluster size is displayed as number of voxels. Coordinates refer to the MNI coordinates.

Figure 1. Overview of the reconstructed white matter tracts.

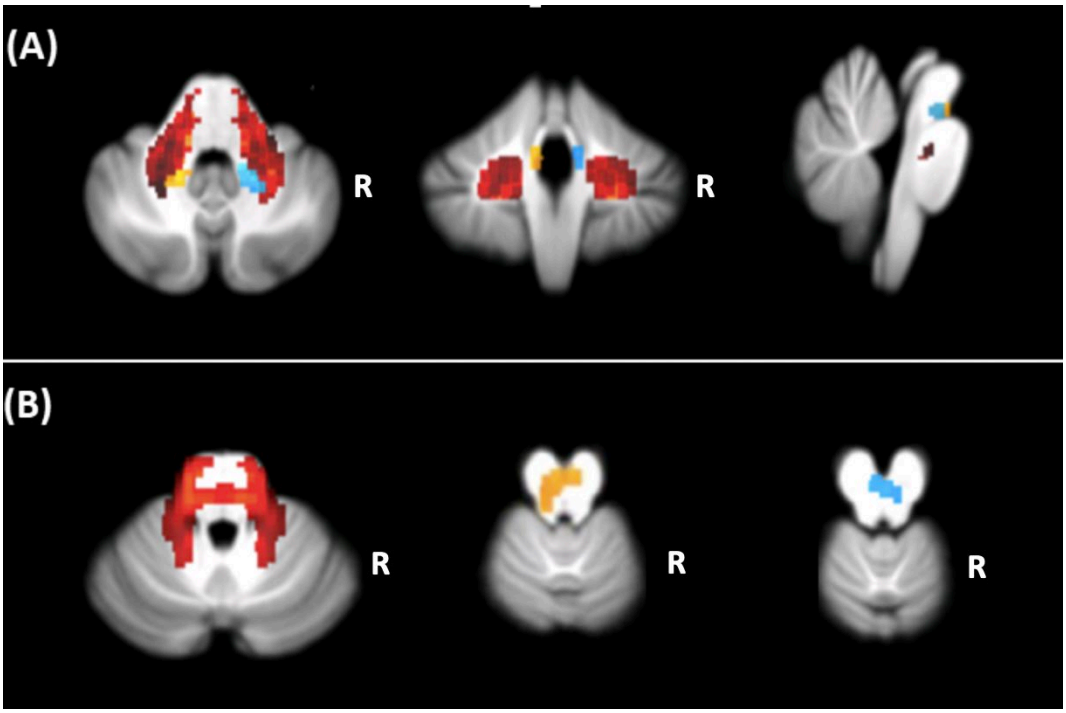

Panel A. Medial Cerebellar Peduncle (MCP) (red); Left Superior Cerebellar Peduncle (LSCP) (yellow); Right Superior Cerebellar Peduncle (RSCP) (light blue).

Panel B. MCP included the transverse pontine fibers posterior and anterior to the corticospinal tracts (red overlay), while the SCP featured a visible decussation at the level of the midbrain: SCPL (yellow overlay); SCPR (light blue overlay).

Figure 2. Voxel-wise correlation between reduced fractional anisotropy in the middle cerebellar peduncle and grey matter atrophy in Lobule IX in AD.